Supplemental material to the article

Alkali metal atoms in strong magnetic field: "guiding" atomic transitions foretell characteristics of all transitions of D1 line

It is worth mentioning that also for lower magnetic field ($B = 4.5\,\mathrm{kG}$) the individual transitions between magnetic sublevels are sufficiently separated to be resolved by $\lambda/2$-method. Fig. 1 below shows experimentally recorded spectrally resolved 10 transitions of high-frequency group (see Fig. 6 in the main text), along with fitting for each individual transition performed using "pseudo-Voigt" function (Microcal Origin 7, PsdVoigt1 function, parameter $\mu = 1.2$).

The spectrum consists of two groups: four transitions labeled as $1'$–$4'$ correspond to ^{87}Rb, and six transitions labeled 1–6 correspond to ^{85}Rb (for labeling, see Fig. 2 in the main text). The "guiding" atomic transitions (GAT) for ^{87}Rb and ^{85}Rb are transitions $4'$ and 6 respectively, which are marked in squares. As is mentioned in the main text, for the case of $B = 6.05\,\mathrm{kG}$ the ratio of square of dipole moment for an individual transition of ^{85}Rb to the corresponding value for GAT is practically equal to 1 (Fig. 4), that is confirmed by the recorded spectra presented in Fig. 7. In the conditions of Fig. 1 above (for weaker magnetic field), this ratio is 0.93, which is consistent with the theory (Fig. 4 of the main text). This behavior is explained by the fact that condition $B \gg B_0$ (i.e. HPB regime) is fulfilled better for $B = 6.05\,\mathrm{kG}$ than for $B = 4.5\,\mathrm{kG}$. The transitions $2'$

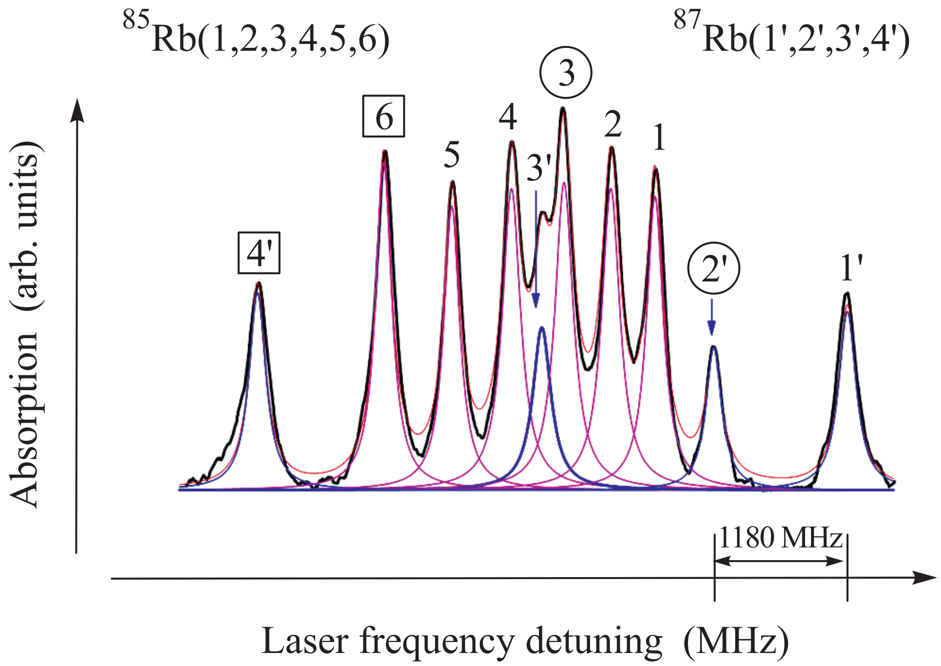

Figure 1: Absorption spectrum of Rb D_1 line (high frequency range) for π-polarized $10\,\mu$W laser excitation, recorded with nanocell of $L = \lambda/2$ thickness at $120\,°$C. The spectrum consists of two groups of transitions between magnetic sublevels: four transitions labeled $1'$–$4'$ (^{87}Rb), and six transitions labeled 1–6 (^{85}Rb). The "guiding" transitions (GAT) for ^{87}Rb and ^{85}Rb are $4'$ and 6 respectively, labeled in squares. The amplitude of GAT is maximal among its group, as is predicted by theory (Fig. 4 in the main text). Transitions labeled $2'$ and 3, which are forbidden $at B = 0$, are marked by circles.

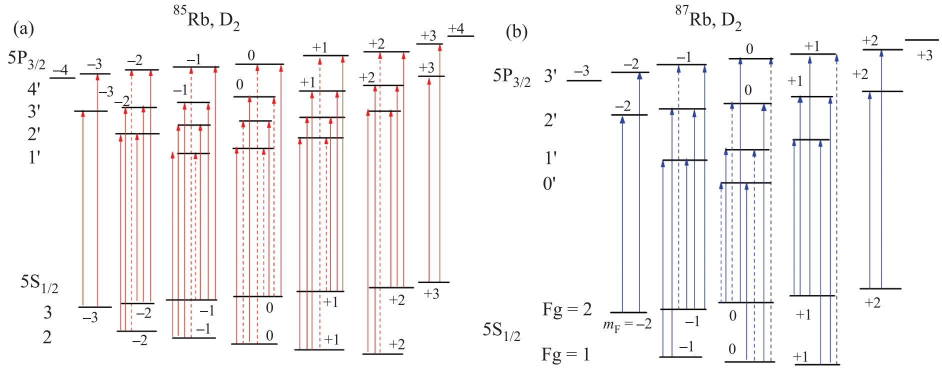

Figure 2: Diagram of hyperfine structure of D$_2$ line of ^{85}Rb (a) and ^{87}Rb (b) in magnetic field, with all the possible transitions between Zeeman sublevels under π-polarized laser excitation. 40 transitions for ^{85}Rb including those forbidden at $B = 0$ ($\Delta F = 0$, $m_F = m_{F'} = 0$ and $\Delta F = \pm 2$), and 24 transitions for ^{87}Rb including those forbidden at $B = 0$ ($\Delta F = 0$, $m_F = m_{F'} = 0$ and $\Delta F = \pm 2$). No guiding transition for D$_2$ line

and 3 labeled in circles are forbidden at $B = 0$. The increase of B-field results in strong increase of probabilities of these transitions. From Fig. 1, for $B = 4.5\,\mathrm{kG}$ the amplitudes ratio is $A_{2'}/A_{GAT} \approx 0.73$ for ^{87}Rb $A_3/A_{GAT} \approx 0.9$ for ^{85}Rb, while the theory predicts ≈ 0.78 and ≈ 0.94 respectively. Theoretical estimates coincide with the experimental results with inaccuracy of 1–7 % depending on atomic transition. Noteworthy that there is no alternative method capable of providing such quantitative information is reported in the available literature.

The diagrams of hyperfine structure of D$_2$ line of ^{87}Rb and ^{85}Rb in magnetic field are presented in Fig. 2, showing also all the possible transitions between Zeeman sublevels for π-polarized laser excitation. The selection rules for transitions are $\Delta F = 0, \pm 1$, $\Delta m_F = 0$ ($\Delta F = 0$, $m_F = m_{F'} \neq 0$) resulting in 40 transitions for ^{85}Rb and 24 transitions for ^{87}Rb. It is clearly seen that as opposed to the case of D_1 line, there are no solitary π-components for any of transitions in any of $\Delta m_F = 0$ transitions (e.g. for $F_g = 3$, $m_F = -3 \rightarrow F_e = 3$, $m_F = -3$ there is transition $F_g = 3$, $m_F = -3 \rightarrow F_e = 4$, $m_F = -3$, and B-field-induced mixing may occur between $F_e = 3$, $m_F = -3$ and $F_e = 4$, $m_F = -3$ sublevels). Therefore, there shall be no GAT for D_2 line.

The hfs energy levels diagram of D_1 line of Na, ^{39}K and ^{133}Cs in magnetic field and all possible atomic Zeeman transitions for π-polarized exciting laser radiation are shown in Fig. 3, Fig. 4, and Fig. 5, correspondingly. As it is seen, each one of Na, ^{39}K, and ^{133}Cs has two GAT.

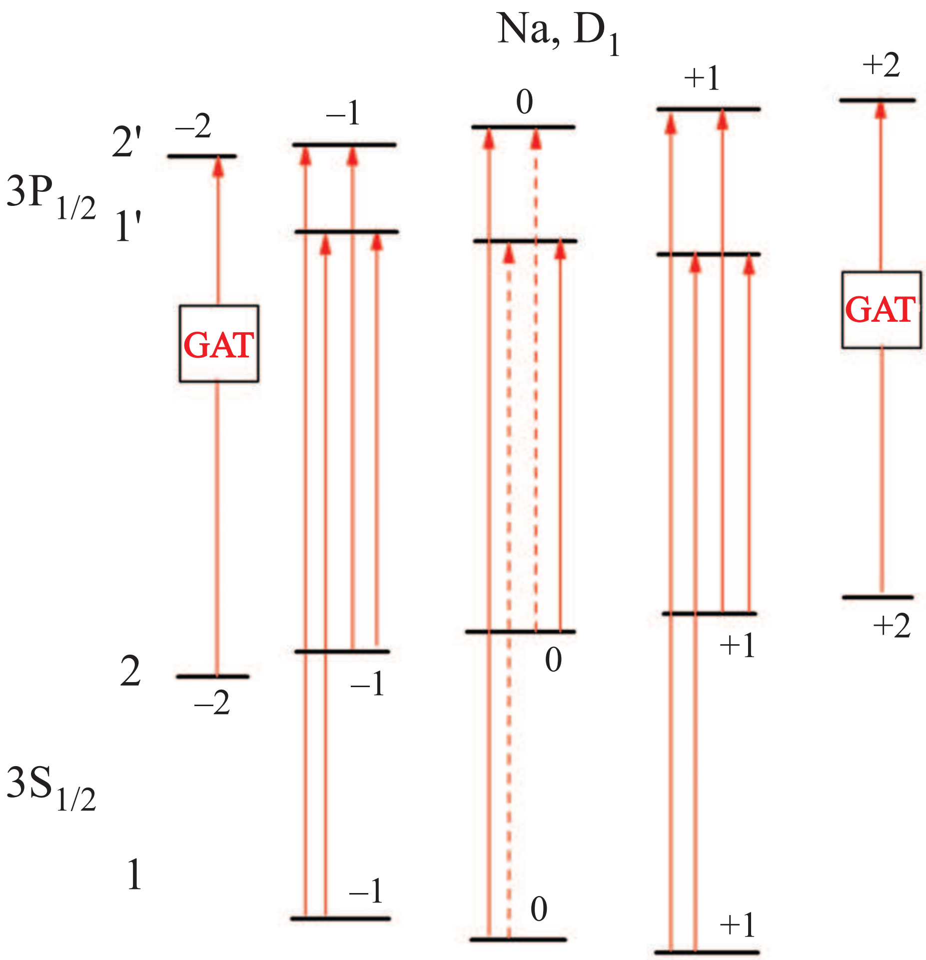

Figure 3: The hfs energy levels diagram of D_1 line of Na atom in magnetic field (for $B < B_0$) and possible atomic Zeeman transitions for π polarized laser radiation excitation are shown. GAT are labeled by rectangles

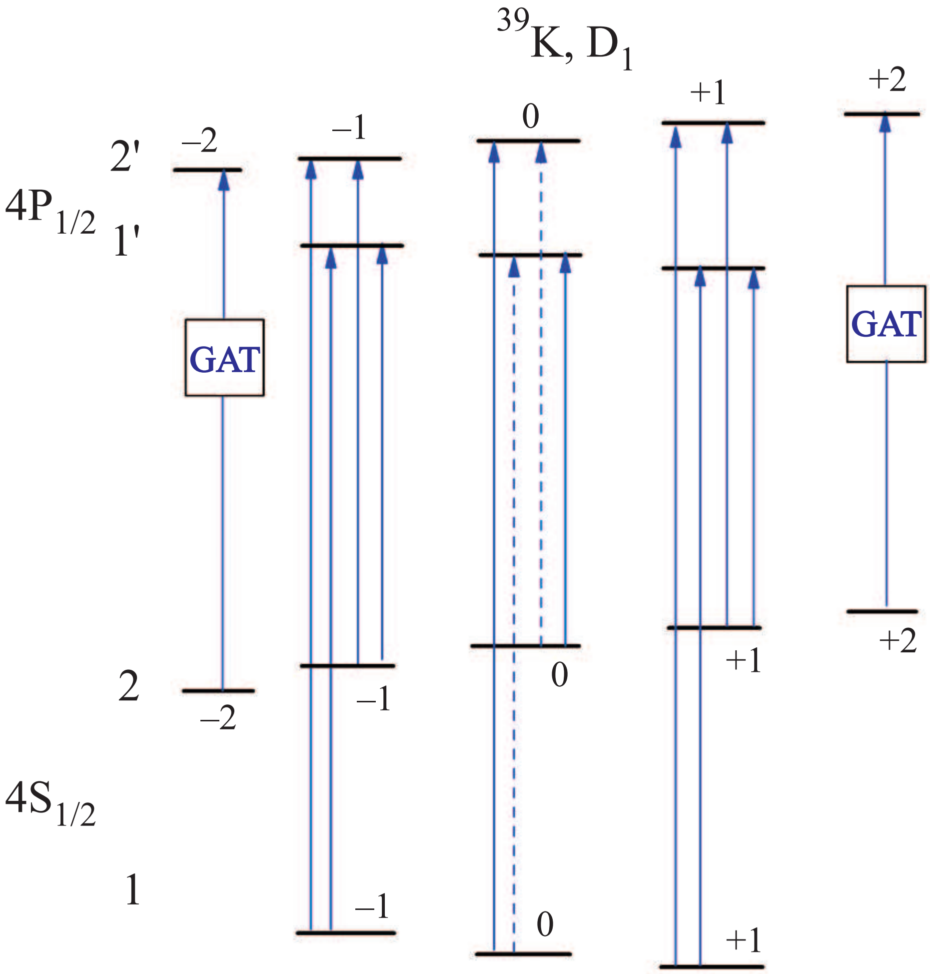

Figure 4: The hfs energy levels diagram of D_1 line of ^{39}K atom in magnetic field (for $B < B_0$) and possible atomic Zeeman transitions for π polarized laser radiation excitation are shown. GAT are labeled by rectangles

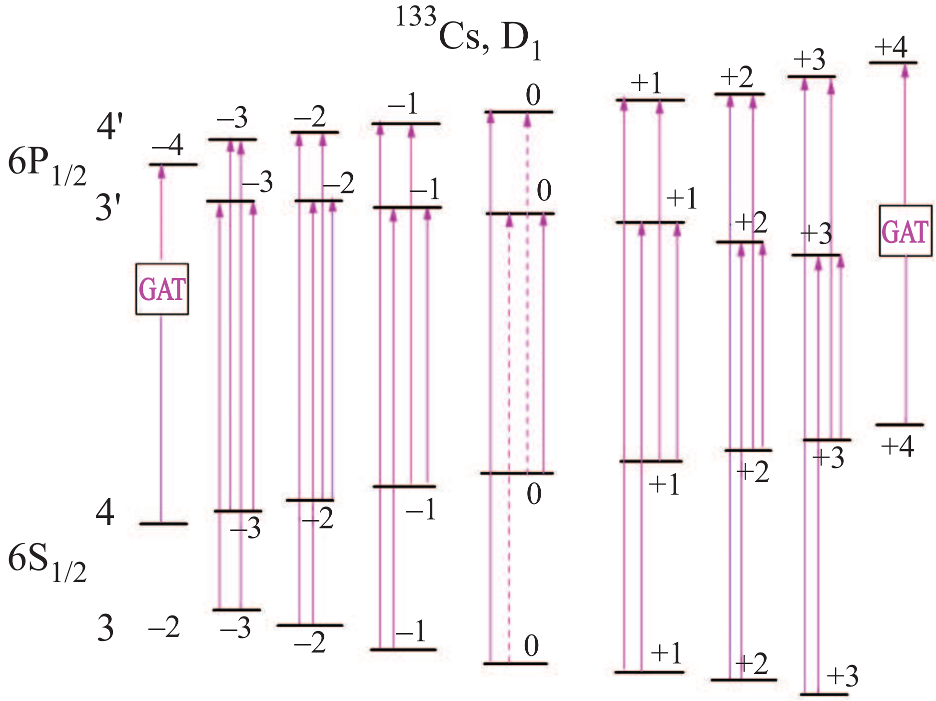

Figure 5: The hfs energy levels diagram of D_1 line of ^{133}Cs atom in magnetic field (for $B < B_0$) and possible atomic Zeeman transitions for π polarized laser radiation excitation are shown. GAT are labeled by rectangles